Proceedings of the 21st ICSMGE, Vienna, Austria, 14 – 19 June 2026. Pistrol, Adam & Schweiger (eds.)
Published by: ÖGG, Austrian Society for Geomechanics, Salzburg, Austria, ISBN 978-3-9503898-4-5
https://doi.org/10.53243/ICSMGE2026-1167

Numerical simulation of driven and bored energy piles in sand under cyclic thermal loading

Bo Sun & Chao Shi
School of Civil and Environmental Engineering, Nanyang Technological University, Singapore, bo007@e.ntu.edu.sg

Anthony Leung
Department of Civil and Environmental Engineering, The Hong Kong University of Science and Technology, Hong Kong, China

ABSTRACT: Although the thermomechanical behavior of bored energy piles has been extensively studied, there is still a knowledge gap concerning on driven energy piles. This study aims to address this gap by developing an effective numerical method to investigate the thermomechanical behaviors of driven and bored energy piles subjected to cyclic thermal loading in sand. The pile-driving process was simulated using the Coupled Eulerian-Lagrangian (CEL) technique, and the post-installation soil state was subsequently mapped onto an axisymmetric finite element model to analyze the thermomechanical response of driven energy piles. In comparison, bored energy piles were wished-in-place and subjected to thermomechanical loading only. The influence of driving depth was also examined through simulations with different driving lengths. Results indicate that the pile-driving process induces significant axial force and negative skin friction along the pile shaft, with the magnitude increasing with greater driving depth. These effects gradually diminish over five heating-cooling cycles. For driven energy piles with a driving depth equal to or greater than one pile diameter, slight heave occurs due to the reduction of downward shaft resistance and minor unloading at the pile toe after thermal cycles. In contrast, when the driving depth is limited to half a pile diameter, driven energy piles exhibit a ratcheting settlement pattern similar to that of bored energy piles, primarily caused by the mobilization of base resistance during thermal cycling.

KEYWORDS: Pile installation, Coupled Eulerian-Lagrangian, hypoplastic model, energy geostructures.

1 INTRODUCTION

Energy piles are innovative foundation elements that integrate structural support and ground heat exchange, offering a sustainable alternative for building heating and cooling by utilizing shallow geothermal energy (Laloui et al. 2006, Yan et al. 2024). Based on construction techniques, energy piles can be broadly categorized into bored and driven types. Bored piles are cast in-situ after inserting reinforcement and heat exchange pipes into pre-drilled holes, while driven energy piles are prefabricated and installed by driving into the ground using hydraulic hammers (Sadeghi & Singh 2023). Despite their advantages in construction efficiency and end-bearing capacity, driven energy piles have seen limited adoption due to insufficient understanding of their long-term thermomechanical behavior under cyclic thermal loading.

The installation process significantly influences the stress and void of surrounding soils, leading to fundamentally different thermomechanical responses between bored and driven energy piles. Previous experimental studies have shown that bored energy piles tend to exhibit irreversible settlement due to thermal cycling (Nguyen et al. 2017), whereas driven piles demonstrate negligible accumulative settlement (Ng et al. 2016, Jiang et al. 2021). However, physical tests mainly provide displacement and temperature data at selected locations, making it difficult to capture stress redistribution and skin friction evolution in the soil-pile interface. As a result, understanding the mechanisms underlying load transfer and deformation remains a challenge.

Numerical simulations offer an effective tool to analyze the full-field thermomechanical response of energy piles. Although extensive studies have investigated bored piles using finite element methods and various constitutive models (Rotta Loria et al. 2015, Ng et al. 2016, Sun & Shi, 2025), research on driven piles remains limited. In particular, few studies have addressed the need to integrate the large-deformation process of pile driving with the subsequent small-strain thermomechanical analysis. This gap hinders the realistic evaluation of driven pile performance subjected to thermal cycles.

To address this issue, this study adopts a recently proposed unified numerical framework for driven energy piles (Sun et al. 2024), which couples the pile driving simulation using the Coupled Eulerian-Lagrangian (CEL) technique with a post-installation axisymmetric model for thermomechanical analysis. This study extends the framework to systematically investigate the influence of driving depth on the thermomechanical behavior of energy piles. A series of simulations with varying driving depths are conducted to identify the threshold depth required to prevent thermally induced settlement. This enhancement provides further insight into the role of installation-induced stress states in shaping long-term energy pile performance under thermal cycling.

2 NUMERICAL MODELING OF DRIVEN AND BORED ENERGY PILES

2.1 *Centrifuge model tests*

Figure 1 presents the schematic layout of the centrifuge model tests conducted by Ng et al. (2016), which served as the experimental basis for validating the numerical models of bored and driven energy piles. The tests were carried out in saturated Toyoura sand with a relative density of 69%. Two model piles were constructed to represent distinct installation methods. The first pile was installed using a "wished-in-place" procedure to simulate a bored energy pile (BEP). The second pile, representing a driven energy pile (DEP), was initially placed at a depth 3D (where D is the pile diameter) shallower than the target depth and then driven to match the embedment level of the BEP. Both model piles were fabricated from aluminum alloy, each with an outer diameter of 19 mm, an inner diameter of 13 mm, and a total length of 600 mm. Ten thermocouples were embedded along the length of each pile at 60 mm intervals. After instrumentation, a 1.5 mm-thick epoxy coating was applied to the pile surface. Additionally, both piles were equipped with internal inlet and outlet ports to enable circulation of the heat transfer fluid. All tests were conducted under a centrifugal acceleration of 40g.

For the BEP test, a constant axial load of 500 N (equivalent to 800 kN in prototype scale) was applied prior to the initiation of five thermal cycles. The initial pile temperature matched the ambient condition of 22 °C, while operating temperatures were varied between 14 °C (cooling) and 30 °C (heating). The DEP test followed a slightly different procedure. The pile was first installed using the "wished-in-place" method and subsequently jacked to the same final embedment depth as the BEP at a constant rate. After pile driving, it was reloaded to 500 N and held under this working load for 2 hours. Once thermal and mechanical conditions stabilized, five thermal cycles were applied in the same manner as the BEP test.

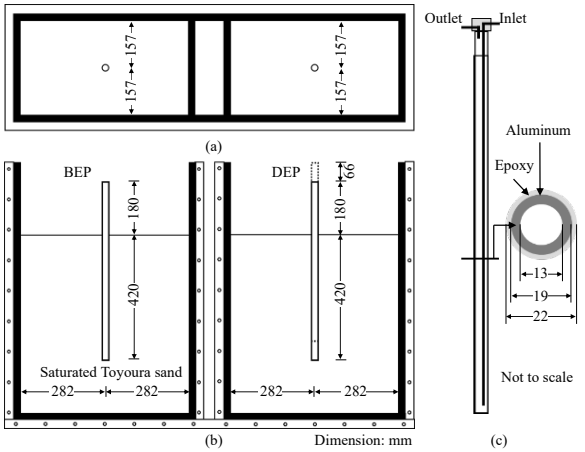

Figure 1. Typical setup of the centrifuge model package: (a) plan view, (b) elevation view and (c) model pile (modified from Ng et al., 2016).

2.2 *Constitutive model for sand*

To accurately simulate the impact of pile installation on the void ratio and stress distribution in sand, an advanced constitutive model is essential. In this study, the hypoplastic model (Niemunis & Herle 1997) was adopted to characterize the mechanical behavior of Toyoura sand. This model is well-suited for capturing the state-dependent and nonlinear response of granular soils. The hypoplastic framework was originally introduced by von Wolffersdorff (1996) and is formulated in terms of the objective stress rate:

$$\mathring{\boldsymbol{T}} = f_s \boldsymbol{L}\colon \boldsymbol{D} + f_s f_d \boldsymbol{N} \parallel \boldsymbol{D} \parallel \tag{1}$$

where $\boldsymbol{L}$ and $\boldsymbol{N}$ are fourth-order and second-order constitutive tensors representing functions of the Cauchy stress $\boldsymbol{T}$; $\boldsymbol{D}$ is the rate of deformation; f_s stands for a barotropy factor accounting for the effect of mean effective stress, and f_d is a pyknotropy factor that relates to the influence of relative density. The original hypoplastic model requires eight material parameters: φ_c', h_s, n, e_{i0}, e_{d0}, e_{c0}, α, and β.

Niemunis & Herle (1997) further extended the hypoplastic model by introducing an intergranular strain concept to better simulate cyclic loading effects. This enhancement involves five additional parameters, i.e. m_R, m_T, R, β_γ, and χ, which govern path-dependent stiffness evolution and the evolution of intergranular strain. The values used in this study for Toyoura sand are summarized in Table 1.

2.3 *Pile installation model*

The installation of driven piles induces large deformations and severe mesh distortion at the pile-soil interface, which conventional FEM schemes struggle to capture effectively. To address this limitation, advanced numerical methods capable of simulating large deformations are required. In this study, the Coupled Eulerian-Lagrangian (CEL) approach was adopted in ABAQUS to simulate pile driving. In the CEL framework, the pile is modeled using rigid Lagrangian elements, while the surrounding soil is discretized with Eulerian elements. Soil-pile interaction is handled within a unified contact algorithm. The Eulerian Volume Fraction (EVF) is used to track soil movement within each cell. The Eulerian time integration algorithm employs a Lagrangian plus remap strategy. In the Lagrangian step, nodes move with the material, allowing the mesh to deform accordingly. This is followed by a remapping step, where the mesh is restored to its original shape and material flow is updated (Pucker & Grabe 2012).

Figure 2 (a) presents the CEL model used in this study. To facilitate prototype-scale simulation, all centrifuge test data (Ng et al. 2016) were converted accordingly, following the "prototype scenario modeling" concept (Rotta Loria et al. 2015). The model pile was assumed to be rigid and non-deformable during installation, with a diameter of 0.88 m (D), a total length of 24 m (27.3 D), and an initial embedment depth of 14.16 m (16 D). The pile was then driven an additional 2.64 m (3 D) into the soil. The soil domain was defined with a radial extent of 6.8 D and depth of 27.3 D. A 1 D-thick void layer was introduced above the ground surface to accommodate soil heave during driving. The pile-soil interface was modeled using a hard contact formulation in the normal direction and a Coulomb friction model in the tangential direction. The groundwater level was assumed to coincide with the ground surface, and the soil was considered fully saturated. Given the high permeability of sand, fully drained conditions were assumed during the analysis, allowing the saturated soil behavior to be approximated using dry sand with equivalent mechanical properties. To improve efficiency, only a quarter-section of the axisymmetric domain was modeled. Fixed vertical and horizontal velocity boundaries were applied at the bottom and sides, respectively. Mesh refinement was employed near the pile to enhance result accuracy while controlling computational cost.

Table 1. Parameters of the hypoplastic model and their values for Toyoura sand (Ng et al. 2016).

Parameter	Symbol	Value
Critical state friction angle	φ_c'	31°
Hardness of granulates	h_s	2.6 GPa
Exponent	n	0.27
Maximum void ratio at zero pressure	e_{i0}	1.10
Minimum void ratio at zero pressure	e_{d0}	0.61
Critical void ratio at zero pressure	e_{c0}	0.98
Exponent	α	0.14
Exponent	β	1.1
Parameter controlling initial shear modulus upon 180° strain path reversal	m_R	11
Parameter controlling initial shear modulus upon 90° strain path reversal	m_T	6
Size of the intergranular strain	R	2×10^{-5}
Parameter controlling the evolution of intergranular strain	β_γ	0.1
Parameter controlling the stiffness degradation with strain	χ	1.0

2.4 *Thermomechanical analysis model*

The thermomechanical behavior of energy piles subjected to cyclic temperature variations involves relatively small strains, which differ fundamentally from the large-deformation conditions during pile installation. In this study, an axisymmetric finite element model was developed using

ABAQUS to investigate the response of energy piles under repeated thermal loading. The pile was assumed to be fully embedded at its final depth, representing the post-installation condition, and was modeled as a linear elastic material to reflect its structural stiffness. The surrounding soil domain was assigned the same radius and depth as in the installation model to ensure consistency in geometric and boundary conditions. The bottom boundary of the model was fixed in the vertical direction, and the lateral boundaries were constrained in the horizontal direction to replicate realistic field constraints. The mesh resolution and element distribution were maintained identical to those used in the pile installation simulation to facilitate the transfer of results between simulations.

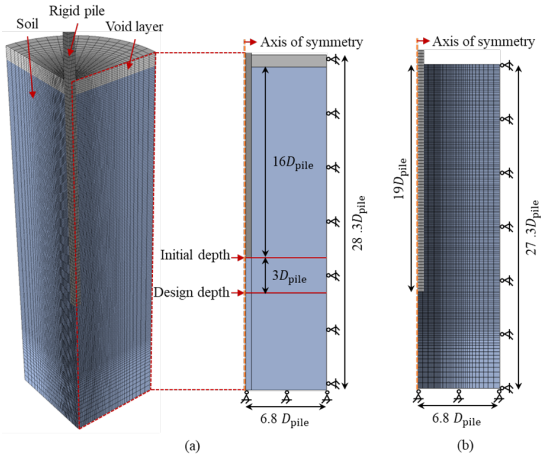

Figure 2. Geometry and mesh of numerical models: (a) pile installation model and (b) thermomechanical analysis model (modified from Sun et al. 2024).

2.5 *Simulation procedures*

For driven energy piles, two distinct numerical schemes were employed to simulate the pile installation process and the subsequent thermomechanical response. The procedure involved four main steps, which are summarized as follows:

(1) The pile installation process was simulated in ABAQUS/Explicit using the CEL technique. After completion, post-installation soil responses were extracted from a vertical section along the axis of symmetry. These responses included stress fields, state variables, and element coordinates.

(2) An axisymmetric thermomechanical (TM) model was developed in ABAQUS/Standard to evaluate the response of the energy pile under cyclic thermal loading using the updated geometry obtained from the CEL simulation.

(3) The post-installation stress and state variables obtained from step (1) were transferred to the TM model developed in step (2). This mapping was performed by establishing spatial correspondences between the two sub-models. The interpolated results were then assigned as initial conditions in the TM model through modifications to the input file (Sun et al. 2024). An unloading step was subsequently introduced to simulate the stress redistribution after jacking, reflecting the start of thermal operation.

(4) Five heating-cooling cycles were applied to the driven energy pile in the TM model to examine its thermomechanical behavior. The temperature histories recorded in the centrifuge tests were directly imposed along the pile shaft, and uniform temperature distribution was assumed in the axial direction.

In addition to the driven energy pile simulations, the thermomechanical response of bored energy piles was also analyzed for validation and comparison. In this case, the simulation bypassed the CEL modeling and relied solely on the TM model. The bored pile was assumed to be wished-in-place to establish the initial geostatic stress field, followed by the application of a constant working load and five thermal cycles.

3 VALIDATION OF NUMERICAL MODELS

The numerical models developed in this study were validated against two centrifuge model tests conducted on driven and bored energy piles. The validation was intended to assess the consistency between the two sub-models, i.e. the CEL model used for simulating pile installation and the TM model for thermomechanical analysis, as well as to evaluate the overall capability of the integrated framework in reproducing the observed thermomechanical responses of both pile types. Details of the model configuration and adopted parameters are summarized in Table 2.

Table 2. Summary of model parameters.

	Parameter	Symbol	Value
Pile properties	Length	L	24 m
	Diameter	D	0.88 m
	Young's modulus	E	27.8 Gpa
	Poisson's ratio	υ	0.33
	Unit weight	γ_p	22.8 kN/m^3
	Linear coefficient of thermal expansion	α_l	4.38×10^{-5}/℃
	Thermal conductivity	λ	54.7 W/m℃
	Specific heat capacity	c_p	863 J/kg℃
Soil properties	Saturated unit weight	γ_s	19.2 kN/m^3
	Linear coefficient of thermal expansion	α_l	1×10^{-5}/℃
	Thermal conductivity	λ	3 W/m℃
	Specific heat capacity	c_p	2239 J/kg℃
Pile-soil interface	Thermal conductivity	λ	3 W/m℃
	Interfacial friction angle	δ	28°

3.1 *Results of pile installation*

Figure 3 presents the post-installation distribution of horizontal stress and void ratio within a typical vertical cross-section along the axis of symmetry. As shown in Figure 3 (a), pile driving induces a significant increase in horizontal soil stress around the pile tip. The horizontal stress exceeds 3 MPa within a radial distance of approximately 3 D and gradually decreases with increasing distance from the pile. Notably, the stress changes are primarily concentrated below a depth of 15 D, while the soil above this depth remains relatively unaffected by the installation process. The left contour displays the horizontal stress obtained from the CEL simulation, while the right contour shows the interpolated values in the TM model. The mapped stress field in the TM model aligns closely with the original CEL results, confirming the accuracy of the solution mapping.

Figure 3 (b) shows the void ratio distribution before and after mapping from the CEL model to the TM model. The initial void ratio of the sand was 0.71, corresponding to a relative density of 69%. Localized densification is evident near the pile toe as a result of pile driving. Similarly, the mapped void ratio field accurately preserves the spatial distribution of the original data, further demonstrating the reliability of the mapping procedure.

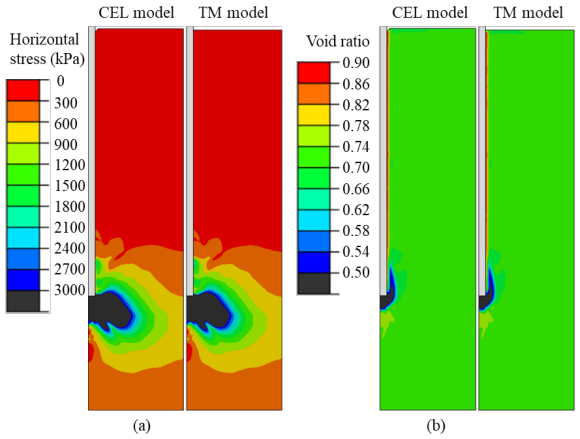

Figure 3. Soil state after pile installation: (a) void ratio; and (b) horizontal stress.

3.2 *Results of pile head displacement*

Figure 4 compares the measured and simulated net head displacement of both bored and driven energy piles after five thermal cycles. Results from centrifuge model tests show that the bored pile experienced progressive settlement, following a ratcheting pattern, with a cumulative displacement of approximately 4.4 D%. In contrast, the driven pile exhibited a slight heave of about 0.4 D% after the same number of cycles.

The numerical simulations successfully captured the overall settlement behavior. For the bored pile, the computed cumulative settlement reached 4.5 D%, closely matching the experimental observations. For the driven pile, both measured and simulated results confirmed that the net vertical displacement remained negligible throughout the thermal loading cycles. These findings demonstrate the capability of the developed finite element models to accurately replicate the thermomechanical response of energy piles installed by different methods in sand.

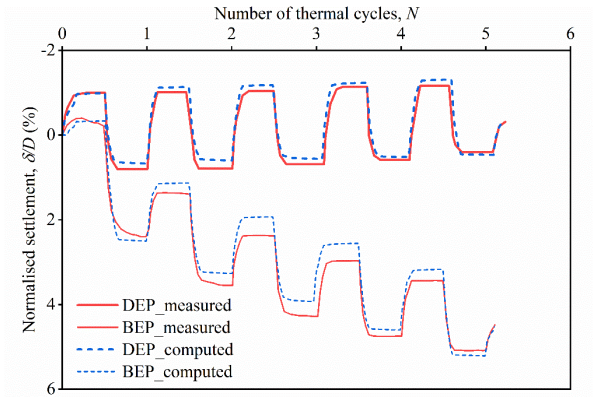

Figure 4. Comparison between measured and computed pile head displacement after five thermal cycles.

4 COMPARISON OF THERMOMECHANICAL BEHAVIOR BETWEEN DRIVEN AND BORED ENERGY PILES

This section presents a comparative analysis of the thermomechanical responses of driven and bored energy piles. To further examine the effect of installation depth on the performance of driven piles, additional simulations were conducted with driving depths of 1 *D* and 0.5 *D*, in addition to the 3 *D* case described in Section 3. For consistency and meaningful comparison, all driven energy piles were subjected to the same working load and thermal loading conditions as the bored energy pile.

4.1 *Comparison of pile head displacement*

Figure 5 illustrates the thermally induced pile head displacements for both bored and driven energy piles under cyclic thermal loading. In general, the heads of all piles exhibit upward movement (heave) during heating and downward movement (settlement) during cooling. The bored pile displays a progressive settlement trend across successive thermal cycles, with the rate of settlement gradually decreasing. This behavior is attributed to increasing soil densification beneath the pile toe during the settlement process, consistent with observations from previous studies (Kalantidou et al. 2012; Ng et al. 2016). After five thermal cycles, the cumulative settlement of the bored pile reaches approximately 4.4 *D*%. The irreversible settlement pattern of the bored pile arises from cyclic shearing and repeated yielding of the surrounding soil, driven by thermal expansion and contraction of the pile. In contrast, the driven pile installed to a depth of 3 *D* exhibits a slight net heave of approximately 0.4 *D*% after five thermal cycles. This upward movement is mainly attributed to unloading in the soil induced by the cyclic thermal loading phase following pile driving.

The displacement behavior of driven energy piles under thermal cycling resembles that of end-bearing piles (Perić et al. 2020). The resistance to settlement is primarily due to localized soil strengthening at the pile base resulting from the driving process, which generates high end-bearing pressure and limits further vertical movement. However, as the driving depth decreases, this restraint effect diminishes. The net heave gradually reduces and transitions into slight settlement. Specifically, after five thermal cycles, a heave of 0.27 *D*% was observed for a driving depth of 1 *D*, while a net settlement of 0.19 *D*% occurred when the driving depth was reduced to 0.5 *D*. These results suggest that, under homogeneous soil conditions, pile driving can significantly reduce long-term displacement due to thermal cycling, provided that the driving depth reaches at least one pile diameter.

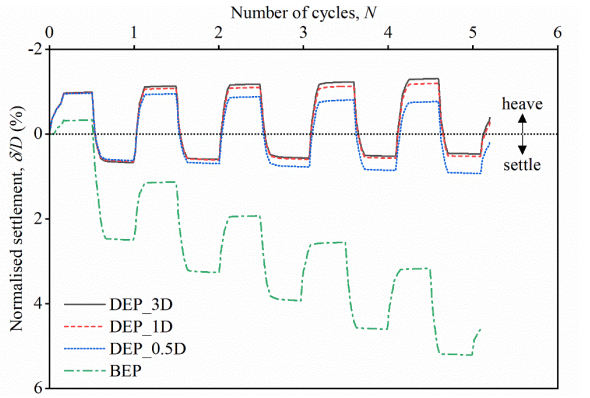

Figure 5. Comparison of thermally induced pile head displacement between driven energy piles and bored energy pile.

4.2 *Comparison of axial load distribution*

Figure 6 compares the axial load distributions along driven and bored energy piles subjected to the same mechanical and thermal loading conditions. Under working load alone, the bored pile exhibits a decreasing axial force profile along its shaft, with a minimum axial force of approximately 210 kN at the pile toe. This pattern reflects typical behavior of semi-floating bored piles, where the downward pile movement relative to the surrounding soil results in positive (upward) shaft resistance (Ng et al., 2015). In contrast, the driven pile demonstrates a substantially different axial load behavior. When driven to a depth of 3 *D*, it develops a toe resistance of approximately 3,895 kN, which is over 18 times greater than that of the bored energy pile. The pronounced end bearing force

is attributed to localized soil densification and strengthening induced by pile driving. As the driving depth decreases, the mobilized toe resistance correspondingly reduces to 2,801 kN at 1 D and 2,101 kN at 0.5 D. This trend highlights the significant role of driving depth in mobilizing end resistance for driven energy piles.

Notably, the axial load in driven piles tends to increase with depth along the shaft under mechanical loading, indicating negative skin friction. This arises from the tendency of the pile to rebound slightly after driving, inducing upward relative movement between the pile and soil, which is a behavior commonly observed in driven piles (Su et al., 2022). In contrast, bored piles experience settlement under loading, which causes downward relative movement and mobilization of positive skin friction along the shaft (Moshtaghi et al., 2023).

After five thermal cycles, both pile types exhibit significant changes in axial load distribution. For the bored energy pile, the axial force at the toe increases to 727 kN, representing a 246% increase compared to the mechanically loaded case. This increase is attributed to enhanced mobilization of end bearing resistance due to continued pile settlement during thermal cycling. The location of the maximum axial load also shifts upward to approximately 10.1 D, which corresponds to the neutral plane, where no relative movement occurs between the pile and the surrounding soil (Shi & Wang 2023). The continued increase in base resistance explains the cumulative settlement observed in Figure 5 and is consistent with the mechanism of progressive mobilization of end bearing capacity (Ng et al. 2016).

In comparison, driven piles initially exhibit much larger axial forces due to soil compaction and stress buildup during installation. However, these elevated axial forces gradually reduce over successive thermal cycles as the soil unloads. This trend corresponds to the observed slight heave in pile head displacement, particularly in the 3 D case shown in Figure 5. As the driving depth decreases, the post-cyclic axial load profiles of driven piles become increasingly similar to those of bored piles. This convergence in behavior reflects the diminishing influence of installation-induced stress when embedment is shallow. From a design perspective, the axial load in driven energy piles tends to decrease over time under cyclic thermal effects. Therefore, short-term axial forces should be considered in reinforced concrete design. Conversely, for bored energy piles, the continuous increase in axial load due to progressive settlement highlights the importance of accounting for long-term loading effects in structural design.

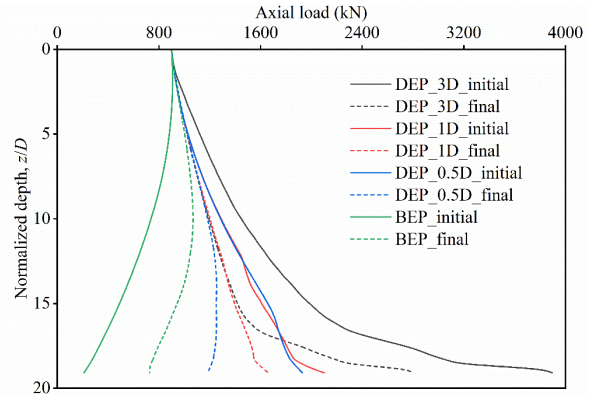

Figure 6. Comparison of axial load distributions between driven energy piles and bored energy pile.

4.3 *Comparison of mobilized skin friction*

Figure 7 presents the distribution of mobilized skin friction along the pile shaft before and after five thermal cycles. A greater driving depth results in a higher magnitude of mobilized skin friction along the driven energy pile, which is attributed to the more pronounced increase in lateral earth pressure at the pile-soil interface induced by deeper pile installation. More importantly, the direction of skin friction differs between the two pile types under the same working load. The driven pile predominantly develops downward (i.e., negative) skin friction, while the bored pile mobilizes upward (i.e., positive) skin friction.

After five thermal cycles, the bored energy pile exhibits negative skin friction above a depth of 8 D, corresponding to the location of the neutral plane, indicating that the pile moves upward relative to the surrounding soil due to thermal expansion. In contrast, driven energy piles continue to exhibit negative skin friction at both 3 D and 1 D driving depths. However, for the pile driven to 0.5 D, the skin friction below a depth of 13 D becomes positive after five thermal cycles. For driven piles with a driving depth equal to or greater than 1 D, significant skin friction develops near the pile toe, which strongly influences subsequent stress redistribution. Due to this substantial shaft resistance, end bearing mobilization during heating and cooling is minimal, explaining the absence of pile settlement. In contrast, for the bored energy pile and the shallowest driven energy pile, settlement is mainly attributed to yielding at the pile toe.

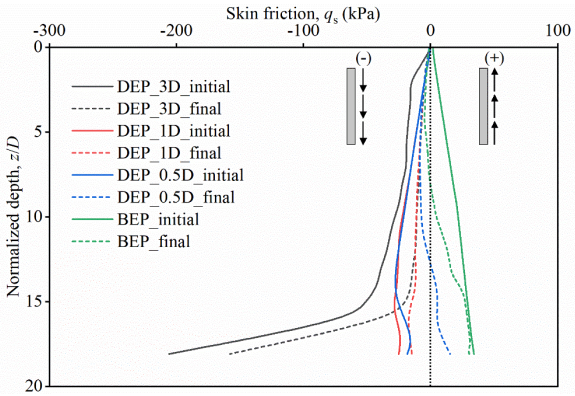

Figure 7. Comparison of skin friction along pile shaft between driven energy piles and bored energy pile.

5 CONCLUSIONS

This study presents a unified numerical framework for investigating the thermomechanical behavior of driven and bored energy piles in sand subjected to cyclic thermal loading. The pile installation process was simulated using the CEL method, and post-installation soil state variables were accurately mapped into an axisymmetric thermomechanical model. Validation against centrifuge model tests confirms the robustness and accuracy of the proposed approach.

Simulation results show that driven energy piles exhibit negligible cumulative settlement under thermal cycles, while bored energy piles experience progressive settlement due to continuous yielding at the pile toe. The direction and magnitude of mobilized skin friction differ between pile types, with significant negative skin friction observed in driven energy piles and positive skin friction in bored energy piles. Driving depth has a significant influence on the thermomechanical response. Deeper driving mobilizes higher shaft resistance and limits thermally induced settlement, whereas shallow driving reduces this effect and results in slight accumulative settlement.

These findings improve understanding of load transfer mechanisms in energy piles under thermal cycling. The proposed framework provides a useful tool for performance-based design, highlighting the importance of accounting for

installation method and driving depth in evaluating long-term serviceability of energy pile systems.

6 ACKNOWLEDGEMENTS

The research was supported by the Ministry of Education, Singapore, under its Academic Research Fund (AcRF) Tier 1 Seed Funding Grant (Project no. RS03/23), AcRF regular Tier 1 Grant (Project no. RG69/23), AcRF Tier 2 Grant (Project No. MOE_T2EP50124-0020), the ASPIRE League Partnership Seed Fund, and the Start-Up Grant from Nanyang Technological University. The financial support is gratefully acknowledged.

7 REFERENCES

Jiang, G., Lin, C., Shao, D., Huang, M., Lu, H., Chen, G. and Zong, C., 2021. Thermo-mechanical behavior of driven energy piles from full-scale load tests. Energy and Buildings, 233, 110668.

Kalantidou, A., Tang, A.M., Pereira, J.-M. and Hassen, G., 2012. Preliminary study on the mechanical behaviour of heat exchanger pile in physical model. Géotechnique, 62(11), 1047–1051.

Laloui, L., Nuth, M. and Vulliet, L., 2006. Experimental and numerical investigations of the behaviour of a heat exchanger pile. International Journal for Numerical and Analytical Methods in Geomechanics, 30(8), 763–781.

Moshtaghi, M., Keramati, M., Ghasemi-Fare, O., Pourdeilami, A. and Ebrahimi, M., 2023. Experimental study on thermomechanical behavior of energy piles in sands with different relative densities. Journal of Cleaner Production, 403, 136867.

Ng, C.W.W., Gunawan, A., Shi, C., Ma, Q.J. and Liu, H.L., 2016. Centrifuge modelling of displacement and replacement energy piles constructed in saturated sand: a comparative study. Géotechnique Letters, 6(1), 34–38.

Ng, C.W.W., Ma, Q.J. and Gunawan, A., 2016. Horizontal stress change of energy piles subjected to thermal cycles in sand. Computers and Geotechnics, 78, 54–61.

Ng, C.W.W., Shi, C., Gunawan, A., Laloui, L. and Liu, H.L., 2015. Centrifuge modelling of heating effects on energy pile performance in saturated sand. Canadian Geotechnical Journal, 52(8), 1045–1057.

Nguyen, V.T., Tang, A.M. and Pereira, J.-M., 2017. Long-term thermo-mechanical behavior of energy pile in dry sand. Acta Geotechnica, 12(4), 729–737.

Niemunis, A. and Herle, I., 1997. Hypoplastic model for cohesionless soils with elastic strain range. Mechanics of Cohesive-frictional Materials, 2(4), 279–299.

Perić, D., Cossel, A.E. and Sarna, S.A., 2020. Analytical Solutions for Thermomechanical Soil Structure Interaction in End-Bearing Energy Piles. Journal of Geotechnical and Geoenvironmental Engineering, 146(7), 04020047.

Pucker, T. and Grabe, J., 2012. Numerical simulation of the installation process of full displacement piles. Computers and Geotechnics, 45, 93–106.

Rotta Loria, A.F., Gunawan, A., Shi, C., Laloui, L. and Ng, C.W.W., 2015. Numerical modelling of energy piles in saturated sand subjected to thermo-mechanical loads. Geomechanics for Energy and the Environment, 1, 1–15.

Sadeghi, H. and Singh, R.M., 2023. Driven precast concrete geothermal energy piles: Current state of knowledge. Building and Environment, 228, 109790.

Shi, C. and Wang, Y., 2023. Stochastic analysis of load-transfer mechanism of energy piles by random finite difference model. Journal of Rock Mechanics and Geotechnical Engineering, 15(4), 997–1010.

Su, D., Wu, Z., Lei, G. and Zhu, M., 2022. Numerical study on the installation effect of a jacked pile in sands on the pile vertical bearing capacities. Computers and Geotechnics, 145, 104690.

Sun, B. and Shi, C., 2025. Interpretable Ensemble Prediction of Thermally Induced Long-Term Pile Settlement from Limited Monitoring Data. Journal of Geotechnical and Geoenvironmental Engineering, 151(9), 04025101.

Sun, B., Shi, C. and Leung, A., 2024. Numerical Investigation on Thermomechanical Behavior of Driven Energy Piles Subjected to Cyclic Thermal Loading in Sand. Computers and Geotechnics, 173, 106582.

von Wolffersdorff, P.-A., 1996. A hypoplastic relation for granular materials with a predefined limit state surface. Mechanics of Cohesive-frictional Materials, 1(3), 251–271.

Yan, Y., Shi, C., Huang, G. and Wang, Y., 2024. Dynamically coupled modelling of ground source heat pump systems considering groundwater flow and unbalanced seasonal building thermal loads. Applied Thermal Engineering, 124713.